Anterior Mitral Leaflet Curvature During the Cardiac Cycle in the Normal Ovine Heart

John-Peder Escobar Kvitting, MD, PhD*; Wolfgang Bothe, MD*; Serdar Göktepe, PhD; Manuel K. Rausch, MSc; Julia C. Swanson, MD; Ellen Kuhl, PhD; Neil B. Ingels, Jr, PhD; D. Craig Miller, MD

Background—The dynamic changes of anterior mitral leaflet (AML) curvature are of primary importance for optimal left ventricular filling and emptying but are incompletely characterized.

Methods and Results—Sixteen radiopaque markers were sutured to the AML in 11 sheep, and 4-dimensional marker coordinates were acquired with biplane videofluoroscopy. A surface subdivision algorithm was applied to compute the curvature across the AML at midsystole and at maximal valve opening. Septal-lateral (SL) and commissure-commissure (CC) curvature profiles were calculated along the SL AML meridian (M_{SL})and CC AML meridian (M_{CC}), respectively, with positive curvature being concave toward the left atrium. At midsystole, the M_{SL} was concave near the mitral annulus, turned from concave to convex across the belly, and was convex along the free edge. At maximal valve opening, the M_{SL} was flat near the annulus, turned from slightly concave to convex across the belly, and flattened toward the free edge. In contrast, the M_{CC} was concave near both commissures and convex at the belly at midsystole but convex near both commissures and concave at the belly at maximal valve opening.

Conclusions—While the SL curvature of the AML along the M_{SL} is similar across the belly region at midsystole and early diastole, the CC curvature of the AML along the M_{CC} flips, with the belly being convex to the left atrium at midsystole and concave at maximal valve opening. These curvature orientations suggest optimal left ventricular inflow and outflow shapes of the AML and should be preserved during catheter or surgical interventions. **(*Circulation*. 2010;122:1683-1689.)**

Key Words: imaging ■ mitral valve ■ physiology

Downloaded from http://ahajournals.org by on July 24, 2020

The shape of the anterior mitral leaflet (AML) changes during the cardiac cycle. As viewed from the left atrium (LA), the systolic shape of the AML along the septal-lateral (SL) meridian (M_{SL}) is concave at the mitral annulus and convex at the central free edge,[1,2] whereas along the central commissure-commissure (CC) meridian (M_{CC}), the AML is concave at both commissures and convex at the belly.[3] During diastole, the AML shape has been described to become convex with respect to the LA along the central M_{SL}[1]; however, no studies describe the diastolic AML shape along the central M_{CC} or the AML shape across the entire AML during the cardiac cycle.

Clinical Perspective on p 1689

A precise characterization of AML shape during the cardiac cycle is clinically important for several reasons. Systolic changes in leaflet curvature could affect left ventricular (LV) outflow profiles. Systolic changes in leaflet curvature could also affect leaflet stress,[4] which, in turn, has been associated with a high recurrence rate of mitral regurgitation after mitral valve repair.[5] In addition, changes in mitral leaflet geometry during diastole could affect transvalvular inflow.[6]

The accurate quantification of leaflet curvature is hampered by the limitations of current imaging modalities. Echocardiography is semiquantitative, requires interpolation of tomographic 2-dimensional planes to construct a 3-dimensional volume of interest, and cannot track distinct anatomic landmarks over time.[7] Magnetic resonance imaging currently has inadequate temporal and spatial resolution to track curvature changes of the mitral leaflets.

We have recently developed a method that enables the characterization and quantification of the curvature of the AML based on Lagrangian coordinates derived from surgically implanted markers using surface subdivision in an experimental ovine model.[8] The surface subdivision algorithm addresses the problem of generating smooth free-form surfaces from arbitrary topologies and allows characterization of curvature profiles for given marker coordinates. In this

Received April 19, 2010; accepted August 13, 2010.

From the Department of Cardiothoracic Surgery, Stanford University School of Medicine, Stanford (J.P.E.K., W.B., J.C.S., E.K., N.B.I., D.C.M.); Department of Mechanical Engineering and Bioengineering, Stanford University School of Engineering, Stanford (S.G., M.K.R., E.K.); and Department of Cardiovascular Physiology and Biophysics, Palo Alto Medical Foundation, Palo Alto (N.B.I.), California.

*Drs Kvitting and Bothe contributed equally to this article.

The online-only Data Supplement is available with this article at http://circ.ahajournals.org/cgi/content/full/CIRCULATIONAHA.110.961243/DC1.

Correspondence to D. Craig Miller, MD, Department of Cardiothoracic Surgery, Falk Cardiovascular Research Center, Stanford University School of Medicine, Stanford, CA 94305-5247. E-mail dcm@stanford.edu

© 2010 American Heart Association, Inc.

Circulation **is available at http://circ.ahajournals.org** **DOI: 10.1161/CIRCULATIONAHA.110.961243**

study, our aim was to quantify the AML curvature of the normal ovine heart over the cardiac cycle using 4-dimensional radiopaque marker tracking and surface subdivision.

Methods

Surgical Preparation

Eleven adult, Dorsett-hybrid, male sheep (weight, 49±4 kg) were premedicated with ketamine (25 mg/kg IM), anesthetized with sodium thiopental (6.8 mg/kg IV), intubated, and mechanically ventilated with inhalational isoflurane (1.0% to 2.5%). All animals received humane care in compliance with the *Principles of Laboratory Animal Care* formulated by the National Society of Medical Research and the *Guide for Care and Use of Laboratory Animals* prepared by the National Academy of Sciences and published by the National Institutes of Health (DHEW NIHG publication 85–23, revised 1985). This study was approved by the Stanford Medical Center Laboratory Research Animal Review Committee and conducted according to Stanford University policy.

Through a left thoracotomy, 13 radiopaque markers were implanted to silhouette the LV at the cross-section points of 2 equally spaced longitudinal and 3 equatorial meridians as described earlier.[9] Using cardiopulmonary bypass and cardioplegic arrest, we sewed 16 radiopaque markers to the mitral annulus, 16 to the AML, and 1 to the central edge of the posterior mitral leaflet (single tantalum loops; 0.6-mm ID, 1.1-mm OD, 3.2 mg each). While intubated and anesthetized, the sheep were immediately transferred with the chest open to the experimental catheterization laboratory.

Data Acquisition and Analysis

Videofluoroscopic images (60 Hz) of the radiopaque markers were acquired with biplane videofluoroscopy (Philips Medical Systems, North America, Pleasanton, Calif). Marker coordinates from 3 consecutive sinus rhythm heartbeats from each of the biplane views were then digitized and merged to yield the time-resolved 3-dimensional coordinates of each marker centroid in each frame with semiautomated image processing and digitization software.[10,11] ECG and analog LV pressure (LVP) were recorded in real time on the video images during data acquisition. These data have served as the basis for other publications from this laboratory.[12,13]

For each beat, end systole was defined as the videofluoroscopic frame immediately preceding the peak negative rate of LV pressure change (−dP/dtmax) and end diastole as the videofluoroscopic frame containing the peak of the R wave on the ECG. The interleaflet distance (defined as distance between the AML central edge and posterior leaflet marker) was plotted throughout the cardiac cycle for each animal (2 consecutive heartbeats). Midsystole for each of these 2 beats was defined from the plotted interleaflet distance curves as follows: [(closure 2−closure 1)/2]+closure 1, where closure 1 is the first time frame of leaflet closure after LV diastolic filling and closure 2 is the time frame immediately before valve opening. The time point of maximal valve opening was determined as the time of maximal interleaflet distance during each heartbeat.

Curvature Analysis

The challenge of the curvature characterization is the generation of a smooth, kink-free surface from the videofluoroscopically determined discrete 23 marker coordinates that define AML geometry. A custom-designed subdivision surface approach was implemented to create a parameterized surface representation of the AML.[8] The algorithm generates an approximating spline patch from the triangulated 23 marker coordinates as the limit of a repeated subdivision using uniform knot intersections. The generation of a smooth free-form surface from discrete data points inherently implies that these points will only be approximated and not interpolated. Accordingly, the experimentally found marker points do not necessarily lie exactly on the approximating subdivision surface; however, computational surface approximation errors have been shown to lie within the range of experimental measurement errors.[8] Overlapping patches of subdivision triangles were used to determine the global second-order continuous curvature field with the help of quartic box splines. Accordingly, the curvature field within each triangle was computed on the basis of the coordinates of the nodes of that triangle and those of its immediate neighbors evaluated over the entire cardiac cycle.[8] To illustrate curvature snapshots at representative time points, individual AML curvature profiles were extracted at midsystole and at maximal leaflet opening for all animals.

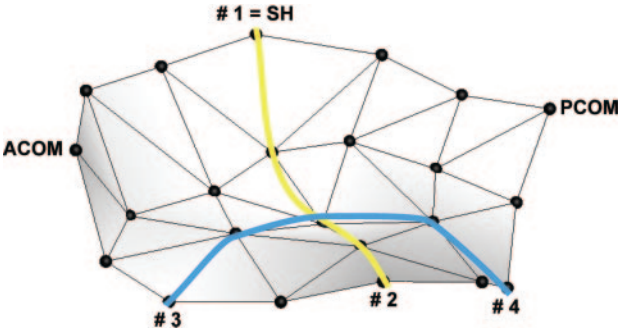

Figure 1. Control mesh based on the implanted surgical markers. The approximation algorithm generates a surface that is C^1 continuous. The yellow line outlines the M_{SL} (between 1 and 2); the blue line, the M_{CC} (between 3 and 4). SH indicates saddlehorn; ACOM, anterior commissure; and PCOM, posterior commissure.

To obtain an impression about the general trend of changes in AML curvature across the entire leaflet at midsystole and at the time of maximal leaflet opening, we present the curvature data as an average over all animals mapped on an averaged leaflet. Because all animals had varying heart rates, the temporal resolution of the acquired data over 1 cardiac cycle varied; to compute averaged curvatures, we aligned all data sets with minimal LVP as the reference point. Subsequently, the marker x,y,z coordinates and the hemodynamic data were normalized. Finally, we performed temporal linear interpolation between the data points to create aligned sets of geometric and hemodynamic data, which were averaged over 1 cardiac cycle, and the calculated curvature was mapped on an averaged leaflet.

The averaged SL curvature values (κ_{SL}) were extracted along an SL AML meridian (M_{SL}) between markers 1 and 2 for 2 heartbeats in each of the 11 individual hearts. The averaged CC curvature values (κ_{CC}) were extracted along a CC AML meridian (M_{CC}) between markers 3 and 4 for 2 heartbeats in each of the 11 individual hearts (Figure 1). A positive curvature was defined as concave toward the left atrium. Data are expressed as mean±SD unless otherwise specified.

The authors had full access to and take full responsibility for the integrity of the data. All authors have read and agree to the manuscript as written.

Results

Hemodynamics

The animals had an average heart rate of 93±10 bpm, dP/dtmax of 1313±315 mm Hg/s, LV end-diastolic volume of 112±13 mL, and maximal LPV of 96±8 mm Hg.

κ_{SL} and κ_{CC} for Each Individual Animal

The leaflet geometries with the corresponding SL and CC curvature contour plots, κ_{SL} and κ_{CC}, for each individual animal at midsystole and at maximal valve opening are shown in Figures 2A, 2B, 3A, and 3B, respectively. These images illustrate not only the interanimal variation in geometry and curvature but also the regional variation of the local curvature distribution.

κ_{SL} Across the Entire AML

Figure 4A and 4B shows average leaflet geometry with the corresponding averaged SL curvature, κ_{SL}, across the entire

Downloaded from http://ahajournals.org by on July 24, 2020

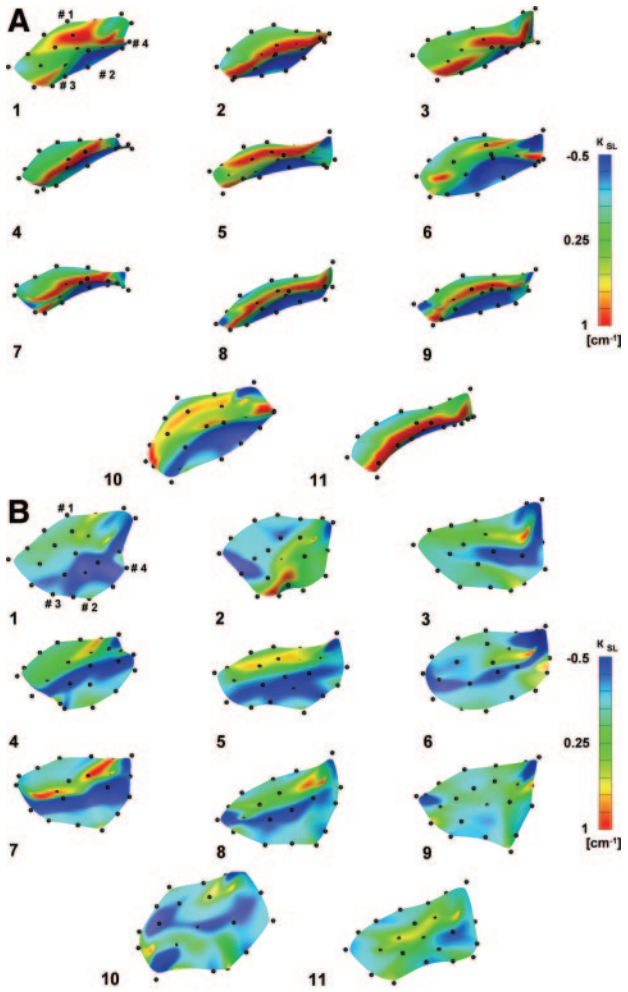

Figure 2. κ_{SL} of the anterior mitral leaflet at midsystole (A) and maximal mitral valve opening (B) for each individual animal, 1 to 11. Marker numbering as in Figure 1.

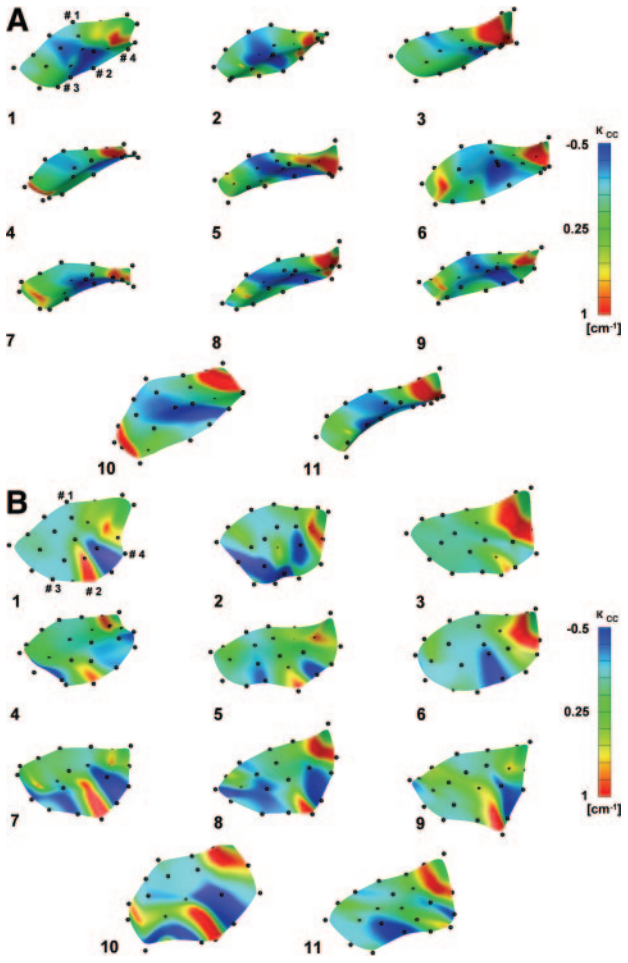

Figure 3. κ_{CC} of the anterior mitral leaflet at midsystole (A) and maximal mitral valve opening (B) for each individual animal, 1 to 11. Marker numbering as in Figure 1.

AML at midsystole and at maximal mitral valve opening, respectively. At midsystole, κ_{SL} is concave with respect to the LA along the entire annular region (green/yellow color code), with the greatest concavity (red color code) in the transitional zone between annular and belly regions. The transitional zone between the belly and leaflet edge regions becomes less concave (green color code) and turns convex toward the leaflet edge region (dark blue color code). At maximal mitral valve opening, κ_{SL} values almost vanish at the annulus and edge regions (light blue color code). The belly is still slightly concave in the transitional zone toward the annulus (green color code) and becomes slightly convex in the transitional zone toward the edge (dark blue color code).

κ_{CC} Across the Entire AML

The CC curvature, κ_{CC}, across the entire AML of the averaged marker coordinates at midsystole and at maximal mitral valve opening is shown in Figure 4C and 4D, respectively. At midsystole, κ_{CC} is concave (green/yellow/red color code) with respect to the LA near the leaflet edge close to the anterior and posterior commissures (3 and 4, respectively). Across the belly, the AML remains mainly concave (green color code) and becomes convex at the central leaflet edge portion (2).

At maximal mitral valve opening, the leaflet is flat along the annulus region (light blue color codes). The belly region of the leaflet toward the central free edge is convex (light blue and dark blue color code) with respect to the LA; this region is flanked on both sides by regions that are concave (green color code) with respect to the LA.

κ_{SL} Along the AML M_{SL}

Figure 5A shows the group mean (±SD) κ_{SL} values along the M_{SL}. At midsystole, described from the saddlehorn marker (point 1) toward the central free edge (point 2), κ_{SL} becomes increasingly concave until it reaches its maximal of 0.98 ± 0.21 cm^{-1} at the transitional zone between the leaflet annular and belly regions (located 0.55 cm from 1; Figure 5A). The curvature values then gradually become less positive and turn negative at the transitional zone between the belly and edge regions. The maximal convexity of -1.1 ± 0.36 cm^{-1} is found close to the AML edge [located 1.78 cm away from the saddlehorn marker (point 1)].

Figure 6B shows the AML κ_{SL} values along the M_{SL} throughout the cardiac cycle (from maximal mitral valve opening to consecutive next maximal opening) for a representative heart. AML κ_{SL} values along the M_{SL} vary significantly between midsystole and maximal valve opening.

Downloaded from http://ahajournals.org by on July 24, 2020

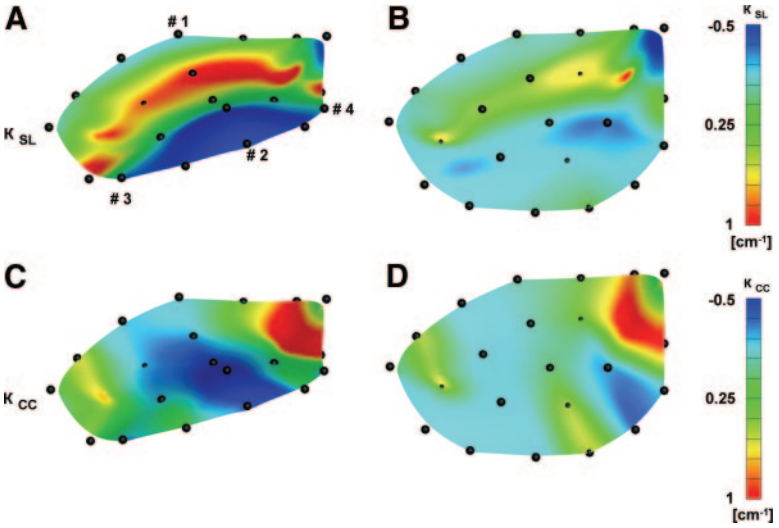

Figure 4. Mean κ_{SL} and κ_{CC} across the anterior mitral leaflet at midsystole (A and C) and maximal mitral valve opening (B and D) averaged from all animals (see Methods). 1 Indicates saddlehorn; 2, central free edge.

κ_{CC} Along the M_{CC}

At midsystole, the group mean (±SD) κ_{CC} values along the M_{CC} (Figure 5B) are positive close to points 3 and 4 (ie, concave with respect to the LA) and negative at the belly (ie, convex with respect to the LA). At maximal opening, the κ_{CC} values along the M_{CC} were reversed, negative near points 3 and 4 and positive at the belly (Figure 5B). The absolute peak average κ_{SL} values along the M_{SL} were approximately triple the absolute peak average κ_{CC} values along the M_{CC}, 1.1±0.36 and 0.35±0.15 cm^{-1}, respectively.

Figure 6C displays the CC curvature, κ_{CC}, along the M_{CC} throughout the cardiac cycle in a representative heart. All but 2 κ_{CC} profiles cluster around 1 configuration in systole and around another one in diastole. The remaining 2 curvature profiles (blue and green lines) are almost completely flat. The first profile (blue) corresponds to mitral valve closure (blue dot in Figure 6A) and the early increase in LVP (Figure 6A). The second profile (green) corresponds to mitral valve opening (green dot in Figure 6A) and the end of the decline of the LVP. The fast curvature flip between systole and diastole is even more evident when the curvature of the entire AML is plotted against the LVP for this heart (see supplemental Movies I and II in the online-only Data Supplement for κ_{SL} and κ_{CC}, respectively).

Discussion

We have shown the 4-dimensional in vivo dynamics of the curvature of the AML based on a dense surgical miniature marker array in an experimental ovine model. In summary, the AML κ_{SL} along the M_{SL} is similarly oriented in the belly region at midsystole and maximal valve opening, with κ_{SL} values being positive near the mitral annulus, ie, concave with respect to the LA, and negative near the edge region, ie, convex with respect to the LA. The κ_{SL} values were higher at midsystole compared with maximal valve opening. In contrast, the AML κ_{CC} values along the M_{CC} in the belly region were negative at midsystole, ie, convex with respect to the LA, but became positive at maximal valve opening, ie, concave with respect to the LA. The magnitude of the κ_{CC} values was similar at midsystole and maximal valve opening. Both the leaflet geometries and the κ_{CC} profiles of the AML along the M_{CC} cluster around 1 configuration in systole and one in diastole, flipping rapidly (≈30 milliseconds) between

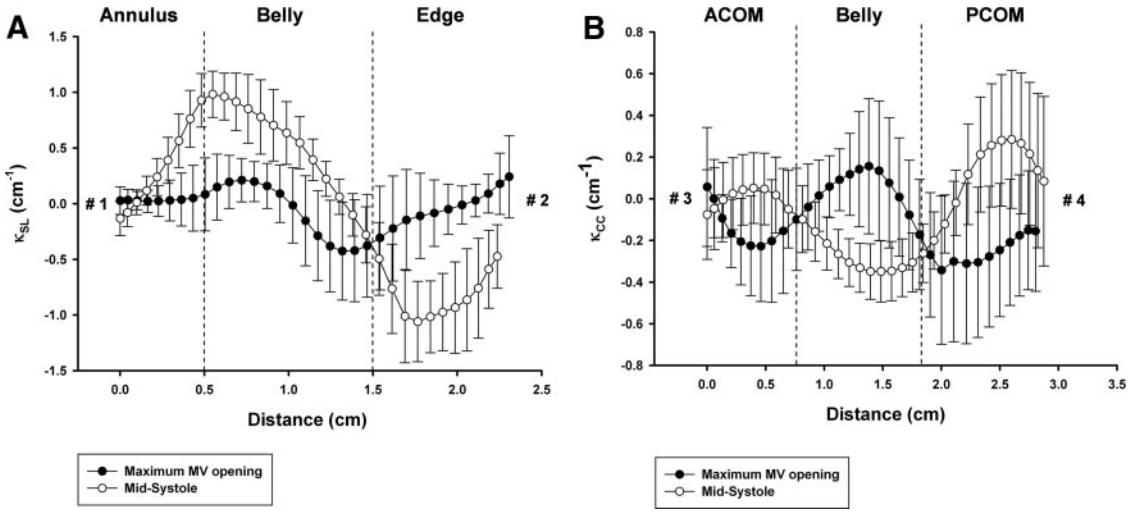

Figure 5. κ_{SL} (A) and κ_{CC} (B) at maximal mitral valve (MV) opening and midsystole. Error bars indicate ±1 SD. 1 Indicates saddlehorn; 2, central free edge; ACOM, anterior commissure; and PCOM, posterior commissure.

Downloaded from http://ahajournals.org by on July 24, 2020

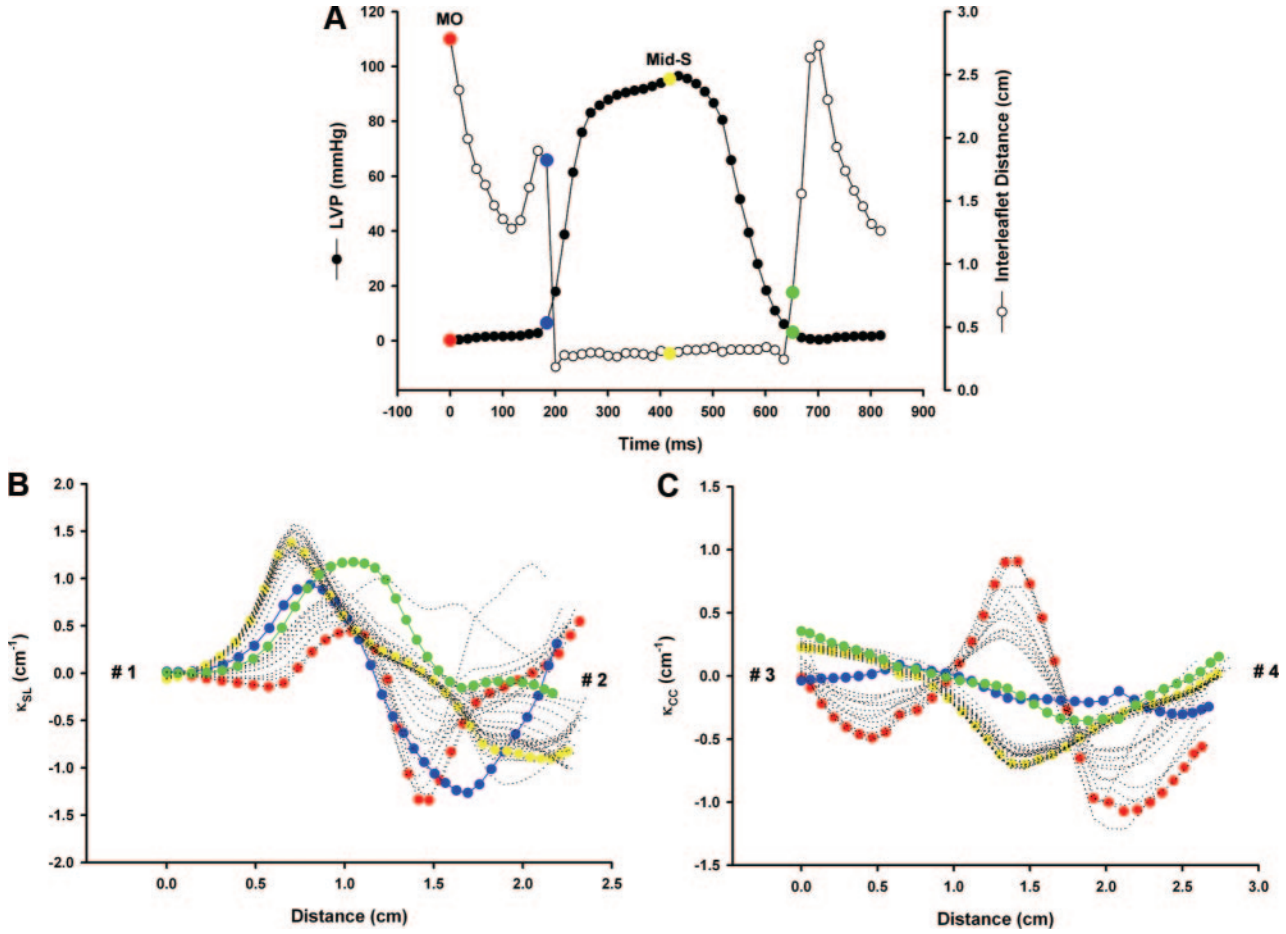

Figure 6. The LVP curve and the distance between the leaflet edge marker of the anterior and posterior mitral leaflet over a cardiac cycle for animal 7 (A). κ_{SL} (B) κ_{CC} (C), where each line represents 1 time step in the cardiac cycle (every 16.7 milliseconds). The red line/dot and the yellow line/dot represent maximal mitral valve opening and midsystole, respectively. The blue line/dot and the green line/dot represent onset of mitral valve closure and mitral valve opening, respectively. 1 Indicates saddlehorn; 2, central free edge.

these configurations. On the contrary, κ_{SL} profiles along the M_{SL} have a much greater variability during each heartbeat.

AML κ_{SL} Along the M_{SL} Is Similarly Oriented in the Belly Region at Midsystole and Maximal Valve Opening

The shape of the M_{SL} during mitral valve closure has previously been described as compound, ie, concave with respect to the LA at the annulus/belly and convex at the edge.[1] In contrast, AML shape has been suggested to be convex with respect to the LA along the entire M_{SL} during valve opening in a recent publication from our laboratory.[13] Surprisingly, we found that the AML curvature along the M_{SL} was compound in the belly region with similarly oriented values at both midsystole and maximal valve opening, with this curvature being more pronounced during midsystole. Expanding on our earlier work in which simple lines were fitted along the M_{SL} from marker to marker, we extrapolated the entire curvature field across the AML. Accordingly, the method used in this article provides a more complete characterization of the AML shape. We hypothesize that the compound shape of the AML belly along the M_{SL} that we observed provides an optimal shape for both systolic outflow and diastolic inflow of blood. Alterations of this shape (eg, in patients with diastolic leaflet tethering) have perturbed LV inflow patterns.[6]

AML κ_{CC} Along the M_{CC} Flips Orientations During Systole and Diastole

In this work, we found that the AML κ_{CC} profile along the M_{CC} flips signs during the cardiac cycle, with the belly being convex and concave with respect to the LA during systole and diastole, respectively. These shape configurations suggest that the AML serves as both an inflow funnel during diastole and an outflow funnel during systole as speculated earlier by Goetz et al.[14] The potential role of the AML as an outflow funnel is further supported by the finding of Walmsley,[15] who described the AML as part of the LV outflow tract in human specimens, ie, as a musculomembranous tunnel, with the interventricular septum anteriorly and the AML posteriorly.

In our study, the location at which the κ_{CC} values change signs along the M_{CC} during systole and diastole (0.8 and 1.9 cm from marker 3 in Figure 3B) correspond approximately to the insertion points of the second-order strut chordae tendinae on the AML. These strut chords have been shown to remain in tension throughout the cardiac cycle[16] and are of key importance in maintaining the systolic and diastolic shape of the AML as demonstrated by Goetz et al.[14] Our results suggest, however, that the strut chords may serve not only as anchors to preserve systolic or diastolic AML shape but also as hinge points for AML shape changes along the M_{CC} during the cardiac cycle.

Downloaded from http://ahajournals.org by on July 24, 2020

Ryan et al[3] used real-time 3-dimensional echocardiography and reported that the κ_{CC} of the AML is negative near the anterior commissure (ie, convex with respect to the LA) becomes positive (or concave) along the belly, and again negative (or convex) near the posterior commissure at end systole. We found a similar curvature configuration at midsystole along the M_{CC}; however, this curvature configuration was reversed at maximal mitral valve opening.

κ_{CC} of the AML Along the M_{CC} Clusters Around 1 Configuration in Diastole and One in Systole, Whereas κ_{SL} Values Along the M_{SL} Have a Much Greater Variability During Each Heartbeat

The present study shows that the κ_{CC} of the AML along the M_{CC} clusters around 1 configuration in diastole and around another one in systole, flipping rapidly between the 2 configurations. κ_{SL} values along M_{SL}, on the contrary, had greater variability (Figure 6 and Movies I and II in the online-only Data Supplement). It seems that the movement of the AML in the CC direction is limited by the secondary strut chords, whereas the leaflet portion along the MSL can move freely without constraints, particularly toward the free edge.

Clinical Inferences

The normal AML curvature may be affected by several interventions such as excision of leaflet material, suture annuloplasty, Alfieri edge-to-edge repairs, or insertion of annuloplasty rings,[17] and differences have been described between flat conventional D-shaped rings and saddle-shaped rings in patients with ischemic mitral regurgitation.[18] The normal ovine curvature data presented here should serve as baseline values for a comparison between different types of annuloplasty rings or surgical repair techniques with respect to their potential effects on AML curvature. In our laboratory, we have conducted a large series of experiments implanting different annuloplasty rings in a releasable fashion,[19] and we are currently investigating ring-induced alterations of the underlying leaflet curvature profiles. Furthermore, our findings suggest that the strut chords may serve not only as anchors to maintain a physiological leaflet shape during systole or diastole but also as hinge points and thus have important implications for leaflet shape changes during the cardiac cycle. Repair techniques that change the geometry and dynamic 3-dimensional motion of the mitral valve have become increasingly popular. For example, results from the Endovascular Valve Edge-to-Edge Repair Study (EVEREST) II clinical trial, in which 279 patients were randomized between conventional open mitral valve repair and the MitraClip (mimicking the surgical Alfieri stitch), were recently reported.[20] This probably affects the dynamic geometric motion of the mitral leaflets during the cardiac cycle and thus perturbs LV inflow and outflow blood flow patterns and strain distributions in the mitral leaflets. Although the effects of a MitraClip or surgical Alfieri stitch on LV blood flow patterns remain to be determined quantitatively in humans, one could speculate that these perturbations might compromise functional clinical outcomes and possibly impair optimal long-term leaflet durability. The normal ovine mitral leaflet curvature observations presented here are important for the understanding and planning of more complex mitral valve repair procedures for patients with ischemic/functional mitral regurgitation. Rodriguez and colleagues[21] showed that cutting second-order chordae changed leaflet curvature along the CC meridian of the anterior mitral valve leaflet; this could augment leaflet stresses and thereby potentially compromise long-term leaflet durability. It is only intuitive and logical that better fundamental understanding of the changes in leaflet curvature during the cardiac cycle in the natural state and after valve repair should spawn more rational valve repair designs, techniques, and devices.

Consequently, interventions should preserve the physiological dynamic curvature patterns reported in this study. Our findings that peak absolute κ_{SL} values are triple the peak absolute κ_{CC} values agree nicely with the findings reported by Sakamoto et al.[22]

Finally, the majority of finite-element models used to study the mitral valve have been based on data from unloaded postmortem specimens or intraoperative observations.[23] The quantitative curvature information provided in this study may help to further refine current finite-element models, especially those that aim to model AML shape throughout the entire cardiac cycle.

Limitations

Our data analyses have several limitations. First, our measurements were obtained in an anesthetized, open-chest ovine model, and our results cannot be translated directly to human pathological conditions. In terms of anatomy, the strut chords are fewer and thinner in sheep, so the curvature surface of the AML could be even more pronounced in humans, as pointed out by Goetz et al.[14] Second, the curvature approximation method used in this experiment is limited by the number of markers implanted; therefore, we might have underestimated the maximal curvature values. Third, the mitral annular and AML marker data were acquired after a brief episode of ischemia and the release of an annuloplasty ring to collect data for another study. These interventions could have influenced our findings. Previous analyses in our laboratory, however, have shown that measurements after transient ischemia were similar to baseline data.[24] Although the κ_{SL} of the AML along the M_{SL} is of similar sign across the belly region at midsystole and early diastole, κ_{CC} along the M_{CC} flips rapidly, with the belly being convex at midsystole and concave at maximal valve opening. These curvature orientations suggest optimal LV inflow and outflow shapes of the AML and should be considered if interventions that may affect the physiological geometry of the mitral valve are performed. Clinical studies are needed to determine the dynamic changes in AML curvature in normal and diseased human hearts.

Acknowledgments

We thank Paul Chang, Eleazar P. Briones, Lauren R. Davis, and Kathy N. Vo for technical assistance; Maggie Brophy and Sigurd Hartnett for careful marker image digitization; and George T. Daughters III for computation of 4-dimensional data from biplane 2-dimensional marker coordinates.

Sources of Funding

The work was supported by US National Institutes of Health grants R01 HL 29589 and R01 HL67025 (Dr Miller); US National

Downloaded from http://ahajournals.org by on July 24, 2020

Science Foundation grant EFRI-CBE 0735551 (Dr Kuhl); Deutsche Herzstiftung (Frankfurt, Germany) research grant S/06/07 (Dr Bothe); the US-Norway Fulbright Foundation, the Swedish Heart-Lung Foundation, and the Swedish Society for Medical Research (Dr Kvitting); and the Western States Affiliate American Heart Association Fellowship (Dr Swanson).

Disclosures

Dr Miller is a consultant for Medtronic Heart Valve Division, Inc and previously consulted for Edwards Lifesciences LLP and Boston Scientific Corp. He is on the Executive Committee of the Edwards Placement of Aortic Transcatheter Valves (PARTNER) trial comparing percutaneous aortic valve replacement methods with conventional aortic valve replacement and has been a speaker at the St. Jude Medical CV Surgical Residents' Symposium. The other authors report no conflicts.

References

1. Karlsson MO, Glasson JR, Bolger AF, Daughters GT, Komeda M, Foppiano LE, Miller DC, Ingels NB Jr. Mitral valve opening in the ovine heart. *Am J Physiol*. 1998;274:H552–H563.
2. Levine RA, Hung J. Ischemic mitral regurgitation, the dynamic lesion: clues to the cure. *J Am Coll Cardiol*. 2003;42:1929–1932.
3. Ryan LP, Jackson BM, Eperjesi TJ, Plappert TJ, St John-Sutton M, Gorman RC, Gorman JH III. A methodology for assessing human mitral leaflet curvature using real-time 3-dimensional echocardiography. *J Thorac Cardiovasc Surg*. 2008;136:726–734.
4. Salgo IS, Gorman JH III, Gorman RC, Jackson BM, Bowen FW, Plappert T, St John Sutton MG, Edmunds LH Jr. Effect of annular shape on leaflet curvature in reducing mitral leaflet stress. *Circulation*. 2002;106:711–717.
5. Jimenez JH, Liou SW, Padala M, He Z, Sacks M, Gorman RC, Gorman JH III, Yoganathan AP. A saddle-shaped annulus reduces systolic strain on the central region of the mitral valve anterior leaflet. *J Thorac Cardiovasc Surg*. 2007;134:1562–1568.
6. Unger-Graeber B, Lee RT, Sutton MS, Plappert M, Collins JJ, Cohn LH. Doppler echocardiographic comparison of the Carpentier and Duran annuloplasty rings versus no ring after mitral valve repair for mitral regurgitation. *Am J Cardiol*. 1991;67:517–519.
7. Mor-Avi V, Sugeng L, Lang RM. Real-time 3-dimensional echocardiography: an integral component of the routine echocardiographic examination in adult patients? *Circulation*. 2009;119:314–329.
8. Göktepe S, Bothe W, Kvitting JPE, Swanson JC, Ingels NB, Miller DC, Kuhl E. Anterior mitral leaflet curvature in the beating ovine heart: a case study using videofluoroscopic markers and subdivision surfaces. *Biomech Model Mechanobiol*. 2010;9:281–293.
9. Timek TA, Dagum P, Lai DT, Liang D, Daughters GT, Tibayan F, Ingels NB Jr, Miller DC. Tachycardia-induced cardiomyopathy in the ovine heart: mitral annular dynamic three-dimensional geometry. *J Thorac Cardiovasc Surg*. 2003;125:315–324.
10. Niczyporuk MA, Miller DC. Automatic tracking and digitization of multiple radiopaque myocardial markers. *Comput Biomed Res*. 1991;24:129–142.
11. Daughters GT, Sanders WJ, Miller DC, Schwarzkopf A, Mead CW, Ingels NB. A comparison of two analytical systems for three-dimensional reconstruction from biplane videoradiograms. *Proc Comp Cardiol (IEEE)*. 1988;15:79–82.
12. Bothe W, Kvitting JPE, Swanson JC, Hartnett S, Ingels NB, Miller DC. Effects of different annuloplasty rings on anterior mitral leaflet dimensions. *J Thorac Cardiovasc Surg*. 2010;139:1114–1122.
13. Bothe W, Kvitting JPE, Swanson JC, Göktepe S, Kathy V, Ingels NB, Miller DC. How do annuloplasty rings affect mitral leaflet dynamic motion. *Eur J Cardiothorac Surg*. 2010;38:340–349.
14. Goetz WA, Lim HS, Pekar F, Saber HA, Weber PA, Lansac E, Birnbaum DE, Duran CM. Anterior mitral leaflet mobility is limited by the basal stay chords. *Circulation*. 2003;107:2969–2974.
15. Walmsley R. Anatomy of human mitral valve in adult cadaver and comparative anatomy of the valve. *Br Heart J*. 1978;40:351–366.
16. van Rijk-Zwikker GL, Delemarre BJ, Huysmans HA. Mitral valve anatomy and morphology: relevance to mitral valve replacement and valve reconstruction. *J Card Surg*. 1994;9:255–261.
17. Ryan LP, Jackson BM, Hamamoto H, Eperjesi TJ, Plappert TJ, St John-Sutton M, Gorman RC, Gorman JH III. The influence of annuloplasty ring geometry on mitral leaflet curvature. *Ann Thorac Surg*. 2008;86:749–760.
18. Vergnat M, Mahmood F, Cheung AT, Khabbaz K, Wiess SJ, Acker MA, Gorman RC, Gorcsan JH III. The influence of annuloplasty ring shape on leaflet curvature in human ischemic mitral regurgitation [abstract E1368]. *J Am Coll Cardiol*. 2010;55:A146.
19. Bothe W, Chang PA, Swanson JC, Itoh A, Arata K, Ingels NB, Miller DC. Releasable annuloplasty ring insertion: a novel experimental implantation model. *Eur J Cardiothorac Surg*. 2009;36:830–832.
20. Cleland JG, Coletta AP, Buga L, Ahmed D, Clark AL. Clinical trials update from the American College of Cardiology meeting 2010: DOSE, ASPIRE, CONNECT, STICH, STOP-AF, CABANA, RACE II, EVEREST II, ACCORD, and NAVIGATOR. *Eur J Heart Fail*. 2010;12:623–629.
21. Rodriguez F, Langer F, Harrington KB, Tibayan FA, Zasio MK, Liang D, Daughters GT, Ingels NB, Miller DC. Effect of cutting second-order chordae on in-vivo anterior mitral leaflet compound curvature. *J Heart Valve Dis*. 2005;14:592–601.
22. Sakamoto H, Parish LM, Hamamoto H, Enomoto Y, Zeeshan A, Plappert T, Jackson BM, St John-Sutton MG, Gorman RC, Gorman JH III. Effects of hemodynamic alterations on anterior mitral leaflet curvature during systole. *J Thorac Cardiovasc Surg*. 2006;132:1414–1419.
23. Arts T, Meerbaum S, Reneman R, Corday E. Stresses in the closed mitral valve: a model study. *J Biomech*. 1983;16:539–547.
24. Glasson JR, Green GR, Nistal JF, Dagum P, Komeda M, Daughters GT, Bolger AF, Foppiano LE, Ingels NB Jr, Miller DC. Mitral annular size and shape in sheep with annuloplasty rings. *J Thorac Cardiovasc Surg*. 1999;117:302–309.

CLINICAL PERSPECTIVE

Anterior mitral leaflet (AML) curvature dynamic changes are of primary importance for optimal left ventricular filling and emptying. Mitral leaflet curvature has been described in the closed position; however, dynamic leaflet curvature has not been characterized. With the increasing use of mitral valve repair techniques that substantially perturb the mitral leaflets (surgical or percutaneous edge-to-edge repair techniques), data describing the 3-dimensional geometry and curvature of the mitral leaflets throughout the cardiac cycle are needed. This in vivo ovine experiment used 4-dimensional tracking of a dense AML marker array coupled with a novel method of surface subdivision to quantify the changes in AML curvature. The septal-lateral curvature of the AML along the septal-lateral meridian was similar across the belly region at midsystole and early diastole; however, the commissure-commissure curvature of the commissure-commissure meridian changes, with the belly being convex to the left atrium at midsystole and concave at maximal valve opening. These findings suggest that the strut chordae may serve not only as anchors to preserve systolic and diastolic AML shape but also as hinge points for AML shape changes along the commissure-commissure meridian. Alteration of the shape of the leaflet could affect diastolic left ventricular filling and theoretically increase leaflet stresses during systole. These data suggest that the natural curvature of the AML produces optimal inflow and outflow shapes of the AML and should be preserved during catheter or surgical repair interventions.

Downloaded from http://ahajournals.org by on July 24, 2020